Eur. Phys. J. A **7**, 279–285 (2000)

THE EUROPEAN PHYSICAL JOURNAL A

Interactions of charmed mesons with nucleons in the $\bar{p}d$ reaction

W. Cassing[1], Ye.S. Golubeva[2], L.A. Kondratyuk[3]

[1] Institut für Theoretische Physik, Universität Giessen, 35392 Giessen, Germany
[2] Institute for Nuclear Research, 60th October Anniversary Prospect 7A, 117312 Moscow, Russia
[3] Institute of Theoretical and Experimental Physics, B. Cheremushkinskaya 25, 117259 Moscow, Russia

Received: 8 November 1999
Communicated by W. Weise

Abstract. We study the possibility to measure the elastic ΦN ($\Phi \equiv J/\psi, \psi(2S), \psi(3770), \chi_{2c}$) scattering cross section in the reaction $\bar{p}+d \to \Phi + n_{sp}$ and the elastic $D(\bar{D})N$ scattering cross section in the reaction $\bar{p}+d \to D^- D^0 p_{sp}$. Our studies indicate that the elastic scattering cross sections can be determined for Φ momenta about 4-6 GeV/c and $D/\bar{D}$ momenta 2 – 5 GeV/c by selecting events with $p_t \geq 0.4$ GeV/c for Φ's and $p_t(p_{sp}) \geq 0.5$ GeV/c for $D/\bar{D}$-meson production.

PACS. 25.43.+t Antiproton-induced reactions – 14.40.Lb Charmed mesons – 14.65.Dw Charmed quarks – 13.25.Ft Decays of charmed mesons

1 Introduction

Apart from the light flavor ($q\bar{q}$) quark physics and their hadronic bound states the interest in hadronic states with strange flavors ($s\bar{s}$) as well as their mutual interactions and properties in the medium has been rising continuously in line with the development of new experimental facilities [1]. In addition to the strange quark sector also the charm quark degrees of freedom have gained vivid interest especially in the context of a phase transition to the quark-gluon plasma (QGP) where charmed meson states should no longer be formed due to color screening [2–4]. However, the suppression of J/Ψ mesons in the high density phase of nucleus-nucleus collisions might also be attributed to inelastic comover scattering (cf. [5–7] and Refs. therein) provided that the corresponding J/Ψ-hadron cross sections are in the order of a few mb [8]. Present theoretical estimates here differ by more than an order of magnitude [9] especially with respect to J/Ψ-meson scattering. Also the $J/\Psi N$ cross section is not known sufficiently well since the photoproduction data suggest a value of 3–4 mb [10], while the charmonium absorption on nucleons (at high relative momentum) in $p + A$ and $A + A$ reactions is conventionally fitted by 6–7 mb [7,11]. In short: the present status of our knowledge on the interaction of charmed mesons with nucleons – especially at low relative momenta – is very unsatisfying.

In this work we explore the perspectives of charmed meson - nucleon scattering in the $\bar{p}d$ reaction because i) antiproton annihilation will produce charmed mesons with rather low momenta in the laboratory and ii) the momentum distribution of the spectator nucleon in the deuteron is very well known. We mention that related experimental studies might be carried out at the future 'glue/charm factory' at GSI that is presently under discussion [12]. An alternative possibility to measure the $J/\Psi N$ elastic scatternig cross section using pion beams in the reaction $\pi^+ d \to J/\psi pp$ has been discussed recently by Brodsky and Miller [13].

Our work is organized as follows: In Sect. 2 we will explore the perspectives for resonance production channels of $J/\Psi, \Psi(2S), \Psi(3770), \chi_{2c}$ and their rescattering on the spectator nucleon including their decay to dileptons. In Sect. 3 nonresonance production channels will be studied in the $\bar{p}d$ reaction with an emphasis on $D\bar{D}$ rescattering and the option to gate on charmonium momenta by triggering on an additional energetic photon or pion. Sect. 4 concludes this study with a summary.

2 Resonance production and rescattering in the reaction $\bar{p}+d \to \Phi + n$

We here examine the possibility to measure the elastic ΦN ($\Phi \equiv J/\psi, \psi(2S), \psi(3770), \chi_{2c}$) scattering cross section in the reaction

$$\bar{p}+d \to \Phi + n_{sp} \to X + n_{sp}, \tag{1}$$

where Φ is produced by resonance fusion $\bar{p}p \to \Phi$ and X the decay product of the resonance. The main contribution to the total cross section of the reaction (1) comes from the spectator term (see diagram a) in Fig 1.), which is dominant if the momentum of the proton-spectator from

[1] supported by DFG, RFFI and Forschungzentrum Jülich.

the deuteron is below 100–150 MeV/c. The amplitude corresponding to the diagram a) of Fig. 1 can be written in the deuteron rest frame as

$$M_a = f(\bar{p}p \to \Phi \to X) \int d^3\ \mathbf{r}\ e^{-i\mathbf{p_2 r}} \Psi_d(\mathbf{r}), \qquad (2)$$

where $f(\bar{p}p \to \Phi \to X)$ is the Breit-Wigner amplitude, $\mathbf{p_2}$ the proton momentum and $\Psi_d(\mathbf{r})$ the deuteron wave function.

Table 1. Charachteristics of the transitions $\bar{p}p \to \Phi$ in vacuum and for a deuteron and carbon target

Φ	J/ψ	$\Psi(2S)$	$\Psi(3770)$	$\chi_{2c}(1p)$
$M_\Phi(MeV)$	3097	3686	3770	3556
$\Gamma_\Phi(MeV)$	0.087	0.277	23.6	2
$k_{cm}(\bar{p}p)(MeV/c)$	1232	1586	1634	1510
$T_{lab}(MeV)$	3250	5400	5700	4845
$Br(\bar{p}p) \times 10^{-4}$	21.4	1.9	2 - 0.2 (?)	1.0
$\sigma(\bar{p}p \to \Phi)(\mu b)$	5.15	0.28	0.7-0.07	0.27
$Br(e^+e^-) \times 10^{-4}$	600	85	0.112	-
$Br(\gamma J/\psi)$	-	-	-	0.135
$S.F.(d) \times 10^{-3}$	1.07	2.6	221	19.2
$S.F.(C) \times 10^{-3}$	0.56	1.24	113	11.2

All resonances $J/\psi, \psi(2S), \psi(3770)$ and χ_{2c} are quite narrow and the decay length for each of them produced in the reaction (1) is much larger than the average distance between two nucleons in a deuteron (see Table 1). Thus the produced meson can rescatter elastically on the neutron spectator, transfering momenta larger than a few hundred MeV/c. In this case the spectator term will become very small and the contribution from the rescattering term become dominant.

Each resonance (produced in the $\bar{p}d$ reaction) has a rather high momentum with respect to the spectator nucleon such that we can describe the rescattering amplitude (see diagram b) in Fig. 1) within the framework of the eikonal approximation (cf. [14–16]) as

$$M_b = -f(\bar{p}p \to \Phi \to X) \int d^3\mathbf{r}\ e^{-i\mathbf{p_2 r}} \Theta(z) \Gamma(\mathbf{b}) \Psi_d(\mathbf{r}), \qquad (3)$$

where the z- axis is directed along the Φ-momentum. The elastic Φn - scattering amplitude is related to the profile function $\Gamma(\mathbf{b})$ by the standard expression

$$f(\Phi n \to \Phi n) = \frac{1}{2\pi i k} \int d^2\mathbf{b}\ e^{-i\mathbf{q b}} \Gamma(\mathbf{b}) \qquad (4)$$

with k denoting the laboratory momentum of the Φ-meson and $\mathbf{q}$ the momentum transfer.

The probability to detect the Φ through the decay channel X at solid angle $d\Omega_d$ in coincidence with the spectator of momentum $\mathbf{p_2}$ is related to the differential cross section as

$$\frac{d^5\sigma(\bar{p}d \to \Phi n \to Xn)}{d\Omega d^3 p_2} = |M_a + M_b|^2. \qquad (5)$$

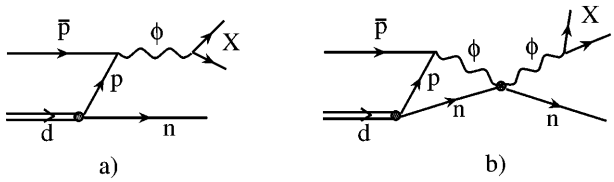

Fig. 1. The diagramms for Φ-meson production in the reaction (1) without (a) and with ΦN rescattering (b)

In order to simulate events for the reaction (1) we use the Multiple Scattering Monte Carlo (MSMC) approach. An earlier version of this approach – denoted as Intra-Nuclear Cascade (INC) model – has been applied to the analysis of η and ω production in $\bar{p}A$ and pA interactions in [17,18]. Recently this version of the INC model has been extended to incorporate in-medium modifications of the mesons produced [19,20] in hadron-nuclear collisions.

However, the INC model is valid only for medium and heavy nuclei and cannot be directly applied to deuterons. In order to perform simulations of scattering events in the case of antiproton – deuteron interactions we use the Monte-Carlo approach for the single and double scattering terms, which are propotional to $|M_a|^2$ and $|M_b|^2$ of (5), respectively. Note that the interference between the spectator and rescattering amplitudes is only important in a narrow region of spectator momenta, where both contributions are of the same order of magnitude. For a more detailed discussion of this point see, e.g., [14–16,21].

The probability for the produced meson to rescatter on the spectator nucleon then can be found in a standard way by

$$W = \frac{\sigma_{el}(\Phi n \to \Phi n)}{4\pi} r_d^{-2} \qquad (6)$$

with

$$r_d^{-2} = \int d^3\ \mathbf{r}\ r^{-2}\ |\Psi_d(\mathbf{r})|^2. \qquad (7)$$

Necessary parameters for a MC simulation of rescattering are the elastic Φn scattering cross sections and slope parameters b for the differential cross sections $d\sigma/dt$, which are approximated by

$$d\sigma/dt = A \exp(bt), \qquad (8)$$

where t is the momentum transfer squared. These parameters as well as the masses of the rescattered particles determine the momentum and angular distributions of the particles in the final state.

An important point for resonance production in $\bar{p}d$ reactions is the rather strong dependence of the Breit-Wigner cross section $|f(\bar{p}p \to \Phi \to X)|^2$ on the initial proton momentum which leads to a rather strong suppression of the cross section on the deuteron or on heavier targets. The suppression factor in the maximum of the cross section is of the order (see [23])

$$S.F. \simeq \pi \Gamma_\Phi m_N / (k_F M_\Phi),$$

where Γ_Φ, M_Φ denote the vacuum width and mass of the produced meson, whereas k_F is the target Fermi momentum. Moreover, after Fermi smearing over the target momentum distribution the Breit-Wigner production cross

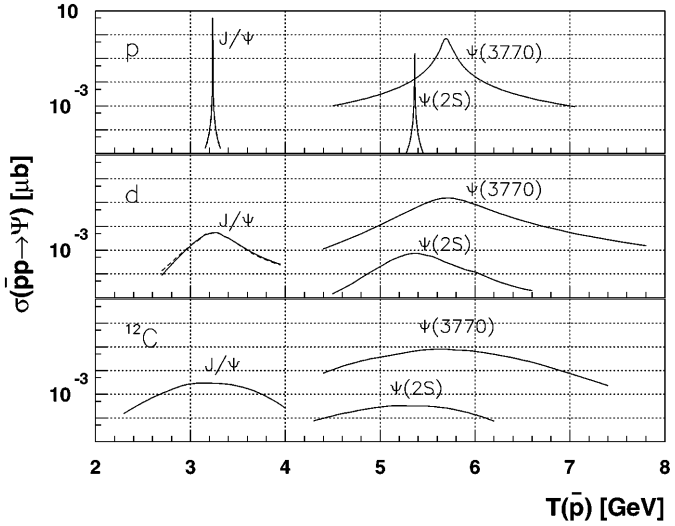

Fig. 2. Fermi smearing of $\sigma(\bar{p}p \to \Phi)$ for $\Phi = J/\psi, \psi(2S)$ and $\psi(3770)$ in deuteron (middle part) and carbon targets (lower part). The upper part shows the elementary cross sections on a hydrogen target

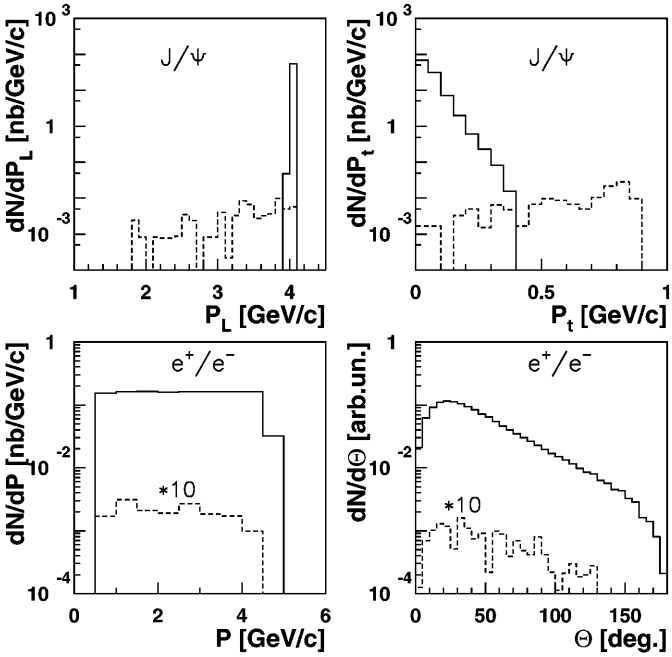

Fig. 3. Distributions of J/ψ mesons from the reaction (10) in longitudinal (upper left) and transverse (upper right) momentum for $T_{lab} = 3.25$ GeV. The distribution of the decay products e^+/e^- in the total momentum is shown additionally (lower left) as well as in the polar angle θ (lower right). The solid and dashed curves describe the contributions of the spectator and rescattering terms, respectively. The $J/\psi n$ elastic scattering cross section was assumed to be 1 mb and the differential slope parameter was taken as $b \simeq 1$ (GeV/c)$^{-2}$

section becomes much wider and asymmetric (see e.g. [22]).

All the effects of Fermi smearing have been taken into account in the MSMC calculations explicitly by convoluting the resonance production cross section with the proton momentum distribution in the deuteron (or heavier nuclei). In a deuteron this distribution is given by the Fourier transformed deuteron wave function squared $|\psi_d(p)|^2$, while in medium and heavy nuclei the local density approximation for the Fermi distribution is used.

In Fig. 2 we present the cross sections $\sigma(\bar{p}p \to J/\psi)$, $\sigma(\bar{p}p \to \psi(2S))$ and $\sigma(\bar{p}p \to \psi(3770))$ as a function of the antiproton kinetic energy for a hydrogen target (upper part), for a deuteron target (middle part) and carbon target (lower part). In Fig. 2 two excitation curves for J/ψ production on the deuteron are shown to demonstrate the dependence on the choice of the deuteron wave function: the dashed line corresponds to the Paris model [24], while the solid curve is calculated using the Hülthen wave function

$$\Psi_d(r) = N\left(e^{-\alpha r} - e^{-\beta r}\right)/r, \tag{9}$$

where N is the normalization factor, $\alpha = \sqrt{m\epsilon} \simeq 46.5\ MeV/c$, $\beta \simeq 5.2\alpha$. One can see that this dependence is quite small since the two results practically overlap.

Let us now consider the reaction

$$\bar{p}d \to J/\psi n \to e^+e^-n \tag{10}$$

In Fig. 3 we show the distributions of J/ψ in longitudinal (upper left) and transverse (upper right) momentum as well as the momentum distribution of the decay products e^+/e^- (lower left) and their distribution in the polar angle θ (lower right) for $T_{lab} = 3.25$ GeV. The solid and dashed curves describe the contributions of the spectator and rescattering terms, respectively. The J/ψ n elastic scattering cross section here was assumed to be 1 mb while the slope parameter was taken as $b \simeq 1$ (GeV/c)$^{-2}$, which is almost the same as in the reaction $\gamma p \to J/\psi p$ [25] at roughly the same $s \simeq 20$ GeV^2.

It is seen that after rescattering on the neutron the J/ψ looses longitudinal momentum (upper left part), but gains transverse momentum (upper right). The momentum spectrum of the leptons from J/ψ decay is completely flat (lower left part), while their angular distribution (lower right) has a broad maximum around 25^o.

It is clear that performing a cut for $p_t(J/\psi) \geq 400$ MeV/c or $p_L(J/\psi) \leq 3.6$ GeV/c one can determine essentially the overall magnitude of the $J/\psi n$ elastic cross section. This is demonstrated in Fig. 4 where we show the number of events as a function of the cut in the J/ψ transverse momentum. The dotted and dashed curves describe the tails of the spectator momentum distribution for the Paris and Hülthen models of the deuteron wave function, respectively. For $p_t(J/\psi) \geq 400$ MeV/c both curves drop far below the solid histograms which describe the contribution of the $J/\psi n$ rescattering term. The relative number of events with rescattering is propotional to $\sigma_{el}(J/\psi n)$ and for the cut $p_t(J/\psi) \geq 400$ MeV/c is about 0.1 % using $\sigma_{el}(J/\psi n) = 1$ mb.

In a similar way we can evaluate the resonance production and rescattering of particles from the Φ family as $\psi(2S)$,$\psi(3770)$ and $\chi_{2c}(1p)$ which can be detected via their decays l^+l^-, $D\bar{D}$ or $\gamma J/\psi$, respectively. The suppres-

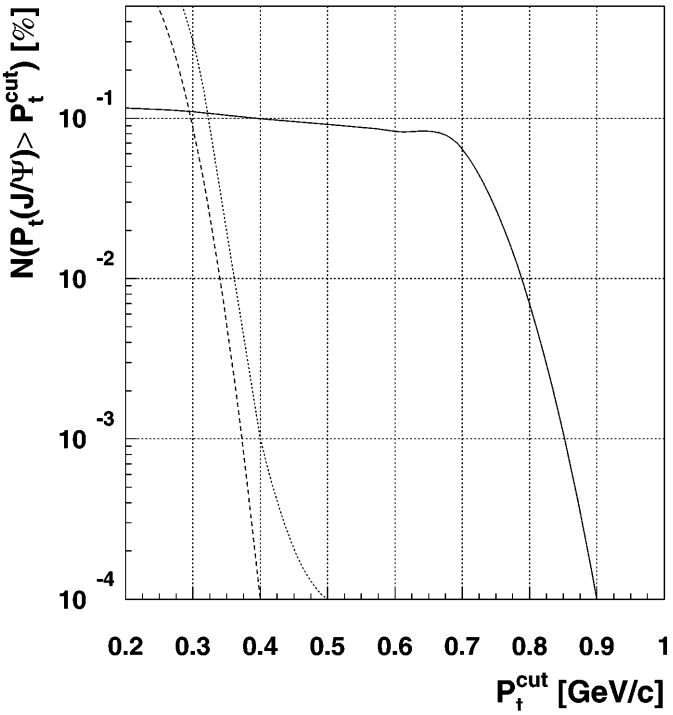

Fig. 4. The number of events for reaction (10) as a function of the p_t cut for $p_t(J/\psi) \geq p_t^{cut}$. The dotted and dashed curves describe the contributions of the spectator term for the Paris and Hülthen models of the deuteron wave function, respectively. The solid curve describes the rescattering term for $\sigma_{el}(J/\psi n) = 1$ mb and a slope parameter for the differential cross section $b = 1$ (GeV/c)$^{-2}$

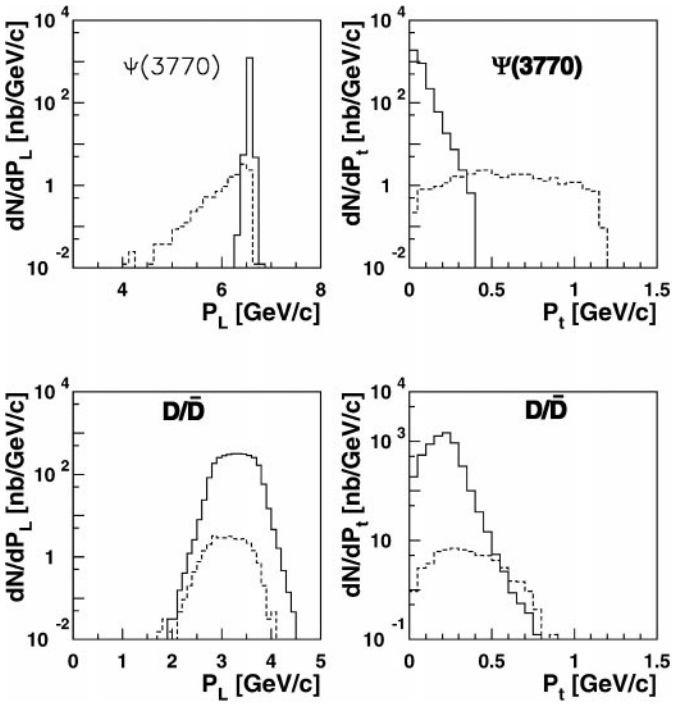

Fig. 5. Momentum distributions in p_L (left) and p_t (right) for $\psi(3770)$ (upper) and $D/\bar{D}$ (lower) from the reaction (11). The solid and dashed curves describe the contributions of the spectator and rescattering terms, respectively, with $\sigma(\bar{p}p \rightarrow \psi(3770))$ =150 nb, $\sigma(\psi(3770)N \rightarrow \psi(3770)N)$ =10 mb and a slope parameter $b(\psi(3770)N$= 2 (GeV/c)$^{-2}$

sion factors due to Fermi smearing of the cross sections $\bar{p}p \rightarrow \Phi$ in deuteron and carbon targets for all particles are shown in Table 1.

The case of the $\psi(2S)$ looks much less promising than the case for J/ψ, because its signal in the l^+l^- channel will be smaller by almost two orders of magnitude. A much stronger signal of the $\psi(2S)$ will be in the channel $J/\psi\pi^+\pi^-$, but in this case a measurement of the $\psi(2S)$ transverse momentum is difficult.

The signal of the $\chi_{2c}(1p)$ in the channel $\gamma J/\psi$ will be almost the same as the signal of the J/ψ in the dilepton channel. Despite of its smaller production cross section in $\bar{p}p$ the $\chi_{2c}(1p)$ is not so strongly suppressed by Fermi smearing as in case of the J/ψ (cf. Table 1). Therefore, if the photon from the $\chi_{2c}(1p)$ decay can be detected in coincidence with the dileptons from the J/ψ decay, a measurement of the $\chi_{2c}(1p)n$ elastic cross section can also be performed by selecting events with $p_t(\chi) \geq 400$ MeV/c.

It is, furthermore, interesting to consider the reaction

$$\bar{p}d \rightarrow \psi(3770)N \rightarrow D\bar{D}N. \qquad (11)$$

Up to now the resonance $\psi(3770)$ has been seen only in the charge neutral mode in e^+e^-- collisions. Therefore, its isospin is not yet known and a detection of $D\bar{D}$ production in $\bar{p}n$ would unambiguously fix its isospin as 1. If the $D\bar{D}$ pair will be produced only on a proton, then its isospin will be 0.

The coupling of the $\psi(3770)$ to the $p\bar{p}$ channel is not known. Having in mind that close to the $\psi(3770)$ the resonances $\chi_{2c}(1p)$ and $\psi(2S)$ have a branching ratio $BR(\bar{p}p) \simeq 2.10^{-4}$ (despite of their full widths being different by almost an order of magnitude), it seems to be justified to assume $BR(\psi(3770) \rightarrow \bar{p}p) \simeq 2.10^{-4} - 2.10^{-5}$. Then the cross section of its production on a nucleon in the deuteron will be about 15–150 nb.

In Fig.5 we present the simulated momentum distributions of $\psi(3770)$ and $D/\bar{D}$ mesons for $\sigma(\bar{p}p \rightarrow \psi(3770))$ =150 nb, $\sigma(\psi(3770)N \rightarrow \psi(3770)N)$ =10 mb and a slope parameter $b(\psi(3770)N)$= 2 (GeV/c)$^{-2}$. The solid and dashed curves describe the contributions of the spectator and rescattering terms, respectively. The $\psi(3770)$ distributions in the longitudinal and transverse momentum are shown in the upper left and upper right part, respectively. The rescattering term dominates for $p_L \leq 6$ GeV/c and $p_t \geq 0.4$ GeV/c. The p_l and p_t spectra of $D/\bar{D}$ mesons are presented in the lower left and lower right part of the figure. The change of the longitudinal and transverse momentum spectra for $\psi(3770)$ due to rescattering has also some influence on the p_l and p_t spectra of the $D/\bar{D}$ mesons especially for the lowest p_l and the highest p_t. However, the signal of rescattering is much cleaner in the p_t distribution of the $\psi(3770)$ for $p_t \geq 0.4$ GeV/c: practically there is no background from the spectator mechanism and the relative number of the events is 0.73 % in case of the cross sections quoted above.

3 Nonresonance production and rescattering of J/ψ and $D/\bar{D}$

Since there is a quite large suppression in the resonance production for narrow quarkonium states on nuclear targets, their nonresonance production (where a suppression factor is absent) might well be comparable to the resonant formation. In this section we thus consider the rescattering of J/ψ and $D/\bar{D}$ in the deuteron where the mesons are produced in the nonresonant reactions

$$\bar{p}d \to J/\psi\ \pi^- p \tag{12}$$

$$\bar{p}d \to J/\psi\ \gamma n \tag{13}$$

$$\bar{p}d \to D\bar{D}N. \tag{14}$$

The cross section of the reaction (14) has been calculated in [26] within the framework of the Quark-Gluon String Model. It grows from threshold up to $p_{lab} \simeq 7.5$ GeV/c, where it reaches its maximal value of about 40 nb, and then decreases rather fast with energy as

$$s^{2[\alpha(0)_{\Sigma_c}-1]},$$

where $\alpha(0)_{\Sigma_c}$ is the intercept of the Σ_c Regge trajectory

$$\alpha(t)_{\Sigma_c} \simeq -1.82 + 0.5t.$$

The cross sections of the reactions (12) and (13) in the continuum are not known. We assume that $\sigma(\bar{p}d \to J/\psi\ \pi^- p)$ is comparable with $\sigma(\bar{p}d \to D\bar{D}N)$ and take for our estimates 30 nb at $T_{lab} = 5$ GeV.

The cross section for the reaction $\bar{p}p \to J/\psi\ \gamma$ can be estimated at $T_{lab} = 4.845$ GeV where it is determined through the resonance $\chi_{2c}(1p)$ (cf. Table 1); it is about 30-40 nb. Of course, in the continuum it is expected to be smaller.

The longitudinal and transverse momentum spectra of J/ψ and the proton spectator from the reaction (12) at T_{lab} =5 GeV are shown in Fig. 6. The solid curves describe the contributions from the spectator term, the dotted and dashed histograms describe the contributions from pion and J/ψ rescattering on the proton spectator. The parameters of the $J/\psi N$ scattering amplitude were taken the same as in Fig. 3. The initial antiproton energy was chosen to be above the $J/\psi\pi$ threshold, but slightly below the $J/\psi\pi\pi$ threshold. Despite the kinematics of the reaction (12) is less restrictive and the J/ψ has a broader distribution in transverse momentum, it is still possible – using the cut $p_t(J/\psi \geq 0.7)$ GeV/c – to obtain a rather clean signal from the $J/\psi N$ rescattering events.

Similar considerations can be made for the reaction (13). In this case it is possible to use the photon momentum as an additional trigger for $J/\psi n$ rescattering events, which can be used to fix the momentum of the J/ψ. The correlation between the longitudinal momenta of J/ψ's and photons is presented for different momenta of the antiproton in Fig. 7 (l.h.s.). As compared to the reaction (12) one looses about 2 orders of magnitude in event rate due to the electromagnetic vertex, but the descrimination

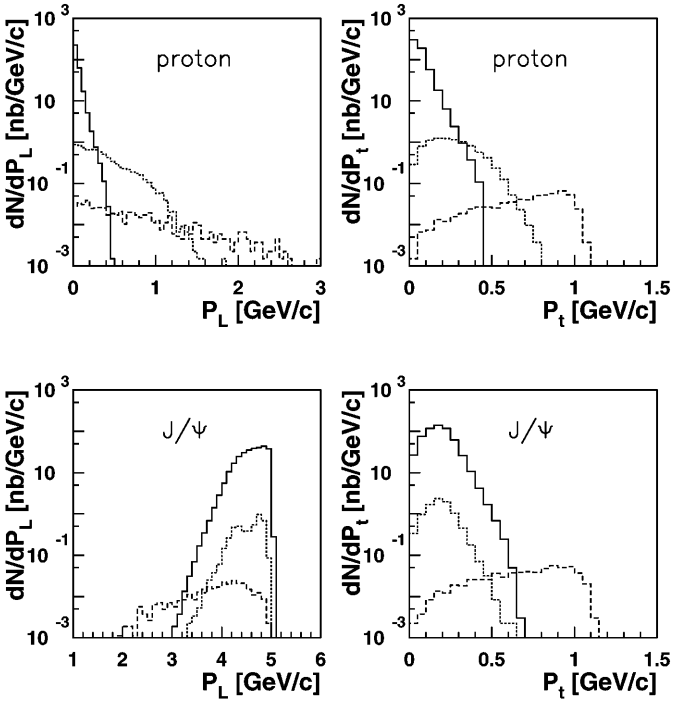

Fig. 6. Longitudinal and transverse momentum distributions of J/ψ (lower part) and the proton spectator (upper part) from the reaction (12) at T_{lab} =5 GeV. The solid curves are the contributions from the spectator term. The contributions from pion and J/ψ rescattering on the proton spectator are shown by dotted and dashed curves, respectively. The parameters of the $J/\psi N$ scattering amplitude were taken the same as in Fig. 3

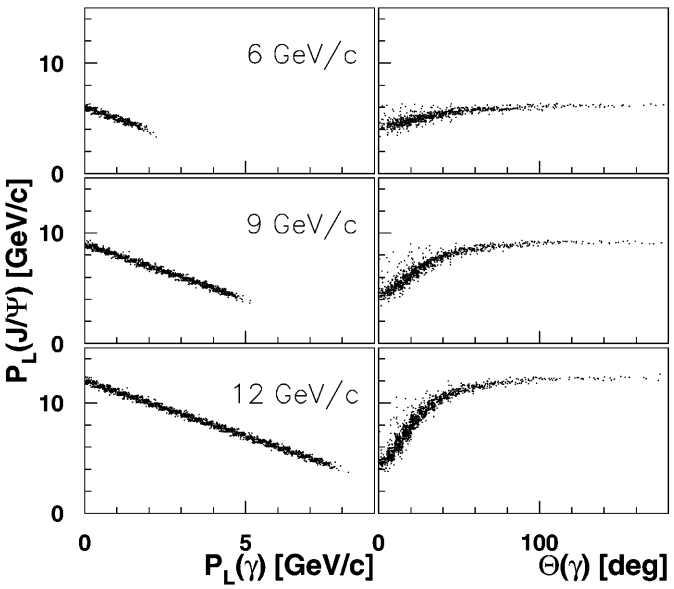

Fig. 7. Correlation between the longitudinal momenta of J/ψ's and photons at p_{lab} = 6, 9 and 12 GeV/c (l.h.s.) and the angular distributions of photons at the same momenta in the reaction (13)

from background events is rather clean. The angular distributions of photons in this reaction are also presented

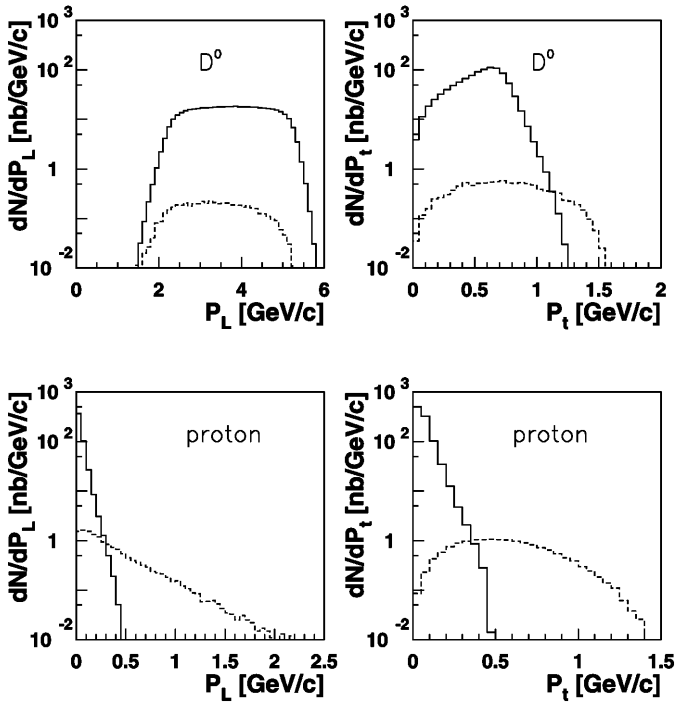

Fig. 8. Longitudinal and transverse momentum distributions of D^0- mesons (upper part) and proton spectators (lower part) from the reaction (14) at p_{lab} =7.5 GeV/c. The solid curves are the contributions from the spectator term while the contributions from D^0N rescattering on the proton spectator are shown by the dashed histograms. The elastic D^0p scattering cross section and the slope parameter b were assumed to be 10 mb and 2 $(\mathrm{GeV/c})^{-2}$, respectively

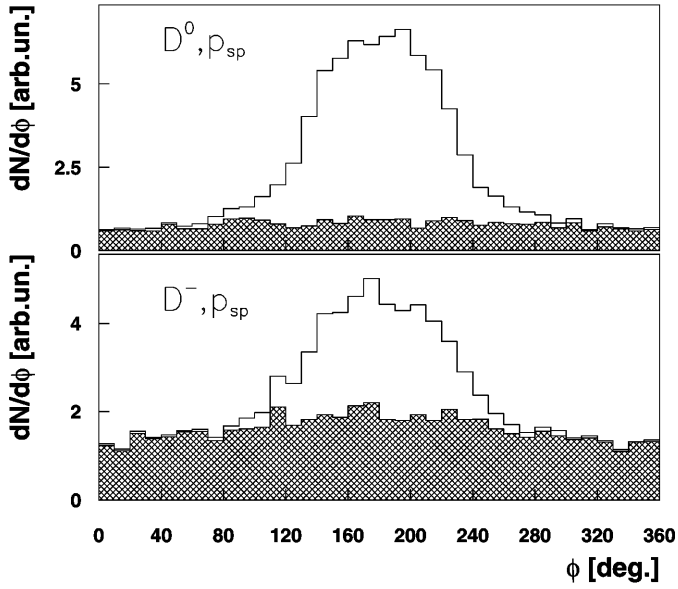

Fig. 9. The distributions in the azimuthal angle ϕ between the planes p_{lab}– p_{D^0} and p_{lab}–p_{sp} (upper part) and between the planes p_{lab}– p_{D^-} and p_{lab}–p_{sp} (lower part) for $p_t(p_{sp}) \geq$ 500 MeV/c in the reaction $\bar{p}d \to D\bar{D}N$ at p_{lab} = 7.5 GeV/c

in Fig. 7 (r.h.s.) and show that the photons are predominantly emitted to forward angles.

Let us now discuss the possibility to measure the DN and $\bar{D}N$ elastic scattering cross sections in the reaction (14). In Fig. 8 we show the longitudinal and transverse momentum distributions of D^0- mesons (upper part) and proton spectators (lower part) at p_{lab} =7.5 GeV/c. The solid curves are the contributions from the spectator term while the contributions from D^0N rescattering on the proton spectator are shown by the dashed histograms. The elastic D^0p scattering cross section and the slope parameter b were assumed to be 10 mb and 2 $(\mathrm{GeV/c})^{-2}$, respectively. In the case of $\bar{D}N$ scattering we have used σ_{el} = 5 mb and the same slope parameter b. In this case the contribution of the D^-p scattering term is smaller by a factor of 2. It is seen that the spectator term dominates for $p_{sp} \leq$ 400 MeV/c. However, at $p_{sp} \geq$500 MeV/c the main contribution to the spectrum comes from the rescattering term. The individual contributions from D^0p and D^-p rescattering can be separated using the correlation between the azimuthal angles of the two scattering planes p_{lab}– $p_{D/\bar{D}}$ and p_{lab}–p_{sp}.

This correlation is presented in Fig. 9 for $p_t(p_{sp}) \geq$ 500 MeV/c where we show the distribution of events in the azimuthal angle between the planes p_{lab}– p_{D^0} and p_{lab}–p_{sp} in the upper part and between the planes p_{lab}– p_{D^-} and p_{lab}–p_{sp} in the lower part. The shaded area describes the background from D^-p (upper part) and D^0p rescattering (lower part).

4 Summary

In this study we have explored the perspectives of measuring the elastic cross section of charmed mesons with the spectator nucleon in resonant and nonresonant $\bar{p}d$ reactions. Our analysis within the MSMC approach indicates that the elastic scattering cross sections can be determined for $\Phi(\equiv J/\psi,\ \psi(2S),\ \psi(3770),\ \chi_{2c})$ momenta about 4-6 GeV/c and $D/\bar{D}$ momenta of 2 – 5 GeV/c by selecting events with $p_t \geq$ 0.4 GeV/c for Φ's and $p_t(p_{sp}) \geq$ 0.5 GeV/c for $D/\bar{D}$-meson production.

We mention that the inelastic cross sections of charmed mesons may be studied in $\bar{p}A$ reactions as analysed in [27]. This opens interesting perspectives for a future high energy antiproton storage ring [12].

We are grateful to A. B. Kaidalov, W. Kühn and A. Sibirtsev for helpful discussions and valuable suggestions. This work was supported by DFG, RFFI and INTAS grant No. 96-0597.

References

1. *Strangeness in Quark Matter 1998*, *J. Phys.* **G 25**, 143 (1999)
2. *Quark Matter '96*, *Nucl. Phys.* **A 610**, 1 (1996)
3. *Quark Matter '97*, *Nucl. Phys.* **A 638**, 1 (1998)

4. T. Matsui, H. Satz, *Phys. Lett.* **B 178**, 416 (1986)
5. W. Cassing and E. L. Bratkovskaya, *Phys. Rep.* **308**, 65 (1999)
6. R. Vogt, *Phys. Rep.* **310**, 197 (1999)
7. X.N. Wang, B. Jacak, eds., *Quarkonium Production in High-Energy Nuclear Collisions*, World Scientific 1998
8. K. Haglin, nucl-th/9907034
9. B. Müller, nucl-th/9906029
10. J. Hüfner and B. Z. Kopeliovich, *Phys. Lett.* **B 426**, 154 (1998); Y. B. He, J. Hüfner, B. Z. Kopeliovich, hep-ph/9908243
11. D. Kharzeev et al., *Z. Phys.* **C 74**, 307 (1997)
12. H. Koch et al., Letter of Intent for the *Construction of a GLUE/CHARM-Factory at GSI*, May 1999, http://www.ep1.ruhr-uni-bochum.de/gsi/part1.ps.gz
13. S. J. Brodsky and G. A. Miller, *Phys. Lett. B* **412**, 125 (1997)
14. L.A. Kondratyuk, *Sov. J. Nucl. Phys.* **24**, 247 (1976)
15. L.A. Kondratyuk and M.Zh. Shmatikov, *Phys. Lett. B* **117**, 381 (1982)
16. A. Bianconi, S. Jeschonek, N.N. Nikolaev and B.G. Zakharov, *Phys. Lett. B* **343**, 13 (1995)
17. Ye.S. Golubeva, A.S. Iljinov, B.Krippa, I.A. Pshenichnov, *Nucl.Phys. A* **537**, 393 (1992)
18. Ye.S. Golubeva, A.S. Iljinov, I.A. Pshenichnov, *Nucl.Phys. A* **562**, 389 (1993)
19. W. Cassing, Ye. S. Golubeva, A. S. Iljinov, L. A. Kondratyuk, *Phys. Lett.* **B 396**, 26 (1997)
20. Ye. S. Golubeva, L. A. Kondratyuk, W. Cassing, *Nucl. Phys.* **A 625**, 832 (1997)
21. V.M. Kolybasov et al., *Phys. Lett. B* **222**, 135 (1989)
22. L.A. Kondratyuk et al., *Nucl. Phys.* **A 579**, 453 (1994)
23. G.R. Farrar, L.L. Frankfurt, M.I. Strikman and H. Liu, *Nucl. Phys.* **B 345**, 125 (1990)
24. M. Lacomb et al., *Phys. Lett. B* **101**, 139 (1981)
25. B. Gittelman et al., *Phys. Rev. Lett.* **24**, 1616 (1975)
26. A.B. Kaidalov and P.E. Volkovitsky, *Z. Phys.* **C 63**, 517 (1994)
27. A. Sibirtsev, K. Tsushima and A. W. Thomas, Eur. Phys. J. **A 6**, 351 (1999)